

Macromolecular Nanotechnology

Morphological effect on spectral property
of poly(9,9-dihexylfluorene-*alt*-2,5-dihexyloxybenzene) films

Meng Wang, Gui-Zhong Yang, Wei-Zhi Wang, Min Wang, Tianxi Liu *

*Key Laboratory of Molecular Engineering of Polymers of Ministry of Education, Department of Macromolecular Science,
Laboratory of Advanced Materials, Fudan University, Shanghai 200433, People's Republic of China*Received 2 February 2007; received in revised form 26 July 2007; accepted 7 September 2007
Available online 15 September 2007

Abstract

In this study the optical property and film morphology of a conjugated polymer, poly(9,9-dihexylfluorene-*alt*-2,5-dihexyloxybenzene) (PF6OC6), are investigated. It is found that the intensity of the 0–1 emission relative to the 0–0 emission in the PL spectra and the full width at the half-maximum (fwhm) of PL spectra of the PF6OC6 films decrease firstly and then increase with increasing the annealing temperature. The polymer films also exhibit different morphological features after annealing at different temperatures. The optical and morphological results suggest that the vibronic structure of PF6OC6 is closely related to the film morphology, and its formation is enhanced in the amorphous (or less ordered) films and inhibited in the ordered films.

© 2007 Elsevier Ltd. All rights reserved.

Keywords: Conjugated polymer; Films; Morphology; Annealing; Photophysics

1. Introduction

Conjugated polymers have attracted extensive attentions for various applications such as field-effect transistors [1–3], photovoltaic cells [4], and light-emitting diodes (LEDs) [5–7] due to their excellent electrical and optical properties, good thermal stability, and ease of processability. In general, most conjugated polymers exhibit well-resolved vibronic structures with 0–0, 0–1 and 0–2 intrachain singlet transitions in their photoluminescence (PL) spectra [8–10]. For example, the emission peaks at

420, 448 and 472 nm of poly(9,9-dialkylfluorene)s correspond to the so-called 0–0, 0–1 and 0–2 transitions, respectively, and its vibronic structure (especially the 0–1 transition) varies with different conditions. Several factors, such as film preparation method [11] and solution concentration [9,12], thermal treatment [13–15], side chain length of polymers [16–18], affect the intensity of 0–1 and 0–2 transitions relative to 0–0 emission, which are usually attributed to intermolecular interaction [19]. For the alternating fluorene–benzene copolymers, the vibronic structure steadily decreases with increasing the length of side chains on phenylene, which is attributed to a reduction of intermolecular interaction [16]. And for the alternating phenoxazine–fluorene copolymers, the PL spectra of polymer films

* Corresponding author. Tel.: +86 21 55664197; fax: +86 21 65640293.E-mail address: txliu@fudan.edu.cn (T.X. Liu).

gradually lose the vibronic structure with increasing the content of phenoxazine in the copolymers, which are assigned to the decrease of intrachain ordering in the copolymers [20]. The effect of applied pressure on the PL properties of conjugated polymer films was reported [21,22]; and for poly(2-methoxy-5-(2'-ethyl-hexyloxy)-*p*-phenylene vinylene) (MEH-PPV) films, the intensity of the 0–1 and 0–2 peaks relative to 0–0 band increased with increasing pressure [9]. These studies indicate that the vibronic structures of conjugated polymers are closely related to the intermolecular interactions, thus to the film morphologies of the polymers. However, direct morphological evidence and detailed investigations about the correlation between the PL behavior and film morphology of conjugated polymers are still lacking.

In this report, the film morphology of poly(9,9-dihexylfluorene-*alt*-2,5-dihexyloxybenzene) (PF6OC6) annealed at different temperatures is investigated using thermal analysis, X-ray diffraction and optical microscopy techniques. And the relationship between the morphology and the vibronic structure of the annealed films is discussed.

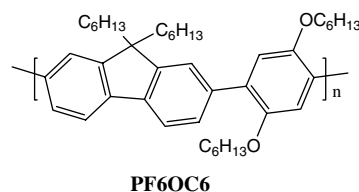
2. Experimental part

2.1. Materials

Poly(9,9-dihexylfluorene-*alt*-2,5-dihexyloxybenzene) (PF6OC6), as shown in Scheme 1, was synthesized with 9,9-dihexylfluorene-2,7-bis(trimethylene boronate) and 1,4-dibromo-2,5-dihexyloxybenzene by Suzuki coupling polymerization according to the literature procedures [23]. All reagents were received from commercial sources and used without further treatment. The pristine films of the synthesized polymer prepared by spin-casting and/or drop-casting from chloroform solution were further annealed at different temperatures for 1 h for subsequent optical, X-ray and microscopy measurements.

2.2. Characterization

Molecular weight was determined by gel permeation chromatography (GPC) with a HP1100 HPLC system equipped with 7911GP-502 and GP NXC columns. The calibration was made with a series of monodispersed polystyrene standards in THF. UV–visible absorption spectra were recorded on a Shimadzu 3150 PC spectrophotometer. Fluorescence measurements were carried out on a Shima-



Scheme 1. Chemical structure of the polymer used.

dzu RF-5301 PC spectrofluorometer with a xenon lamp as a light source. Photoluminescence quantum efficiency (PLQE) measurements were made using a calibrated integrating sphere coupled via an optical fiber linked to a scanning monochromator with a photomultiplier detector. The samples were excited with the 374 nm Zolix PHLM-2 laser. Thermogravimetric analysis (TGA) was conducted on a Shimadzu DTG-60H under a heating rate of 10 °C/min in both nitrogen and air. Differential scanning calorimetry (DSC) was performed on a Shimadzu DSC-60A at a heating rate of 10 °C/min and a cooling rate of 5 °C/min in nitrogen atmosphere. Polarized light microscopy (PLM) images were recorded on LEICA DM LM/P polarized light microscope. X-ray diffraction (XRD) measurements were carried out at room temperature using a Bruker Nanostar U System, with incident X-ray wavelength ($\lambda = 0.1542$ nm). The collimation system consists of two cross-coupled Gobel Mirrors and 4 pinholes. A Histar 2D area detector (Siemens) filled with pressurized xenon gas was used to record the one-dimensional (1D) XRD patterns at voltage of 40 kV and current of 40 mA.

3. Results and discussion

The number-average (M_n) and weight-average (M_w) molecular weights of PF6OC6 were determined to be 17,500 and 28,000, respectively, by gel permeation chromatography (GPC) using polystyrene as the standard. PF6OC6 is air-stable and can be stored without any special precaution. In addition, it exhibits excellent thermal stability, and its thermal decomposition temperature (at 5% weight loss) by TGA is 405 °C and 393 °C in nitrogen and air atmospheres, respectively. PF6OC6 is a good blue light-emitting material. Its chloroform solution exhibits an absorption maximum at 370 nm and a PL emission maximum at 415 nm with a distinct shoulder peak at 440 nm. Compared with the spectra of the solution, the absorption max-

imum of the solid film red-shifts by about 12 nm and the PL emission maximum red-shifts by about 5 nm. And the shoulder peak around 440 nm was also observed in the PL spectra for PF6OC6 film. The maximum peak at 415 nm and the shoulder peak at 440 nm are assigned to 0–0 and 0–1 intra-chain singlet transitions, respectively [8]. The emission spectra indicate the presence of a well-defined vibronic structure for PF6OC6 film. Its photoluminescence quantum yields of the chloroform solution and the film are estimated to be 49.2% and 40.9%, respectively.

Fig. 1 shows the DSC curves of PF6OC6. The first heating curve shows a broad exothermic crystallization peak whose onset is at about 75 °C. In addition, two endothermic peaks are observed at about 127 °C and 142 °C, respectively. Upon the second heating, a distinct step drop is observed at about 67 °C, which is assigned to be the glass transition temperature. Additionally, an exothermic recrystallization peak at about 114 °C is observed. However, only one endothermic peak at about 129 °C is observed and the endothermic peak at 142 °C disappears. And no any phase transition was observed during the cooling scan from the isotropic melt to the ambient. By combining the above DSC results with hot-stage PLM images (not shown here for short), the endothermic peak at lower temperature (127 °C) could be attributed to the phase transition from one crystalline phase (Cr1) to

another one (Cr2) (Cr1 → Cr2); and the peak at 142 °C could be assigned to the phase transition from crystalline to nematic liquid crystalline state (Cr2 → N), and the nematic phase still exists even after starting decomposition. The phase transition behavior and morphology of fluorene-*alt*-benzene based copolymers were detailedly investigated in our previous report [24]. Therefore, the DSC results suggest that the morphology of the PF6OC6 films changes with the temperature.

Based on the DSC results, the PF6OC6 films were annealed in the air at different temperatures for 1 h, and then their PL spectra were characterized. Fig. 2a and b show the PL spectra and the full width at the half-maximum (fwhm) of the annealed films, respectively. It can be seen that the intensity

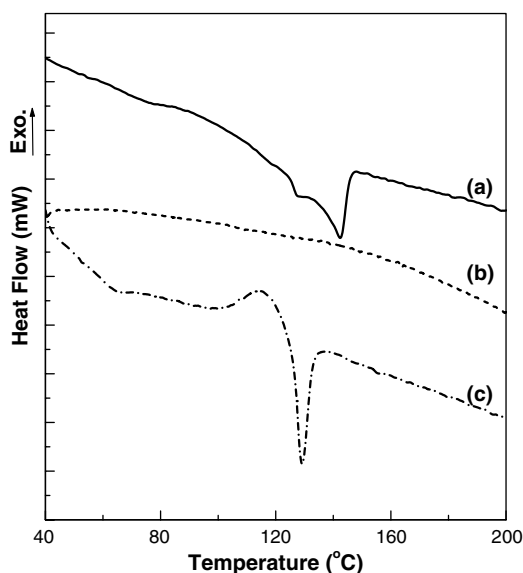


Fig. 1. DSC thermograms of PF6OC6: (a) the first heating, (b) the cooling, and (c) the second heating.

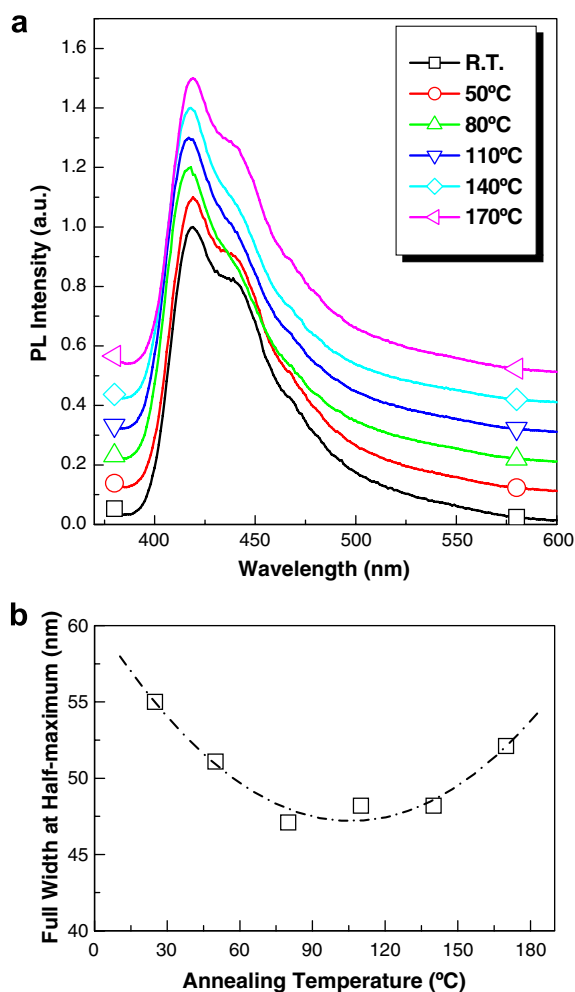


Fig. 2. PL spectra (a) and the full width at the half-maximum (fwhm) (b) of the pristine cast film and the PF6OC6 films annealed at different temperatures.

of 0–1 emission (at about 440 nm) relative to 0–0 emission (at about 415 nm) of the annealed films first decreases with increasing the annealing temperature, and then gradually increases when further increasing the annealing temperature, as shown in Fig. 2a. Interestingly, the fwhm of the PL spectra first increases and then decreases with increasing the annealing temperature, which is consistent with the case of the intensity of the 0–1 emission. And the lowest value of fwhm is observed at about 106 °C. Therefore, it suggests that the change of vibronic structure is closely related to the annealing temperature (thus film morphology) for PF6OC6. Fig. 3 shows the photoluminescence quantum efficiency (PLQE) of the PF6OC6 films annealed at different temperatures. It can be seen that the PLQE of the annealed films remains almost constant with varying the annealing temperature.

In order to further investigate the film morphology of PF6OC6 after thermal treatment, XRD and PLM experiments were carried out. Fig. 4 shows the XRD patterns of the pristine films by drop-casting and the annealed films. For the pristine film (R.T.), only two very broad and diffused scattering peaks were observed, indicating a disordered structure. The XRD pattern of the film annealed at 50 °C (which is lower than the glass transition temperature, 67 °C) was quite similar to that of the pristine film. With increasing annealing temperature to 80 °C, several reflection peaks were observed at 2θ angles of about 5.4°, 6.9°, 10.0° and 14.7°, suggesting formation of an ordered structure. When the annealing temperature was up to 110 °C (which was very close the temperature with the lowest value

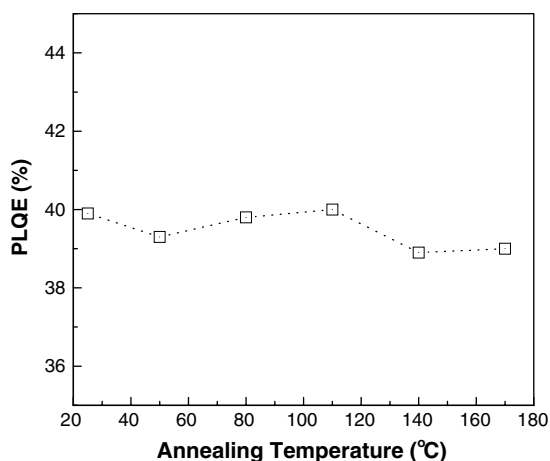


Fig. 3. The PLQE of the films annealed at different temperatures.

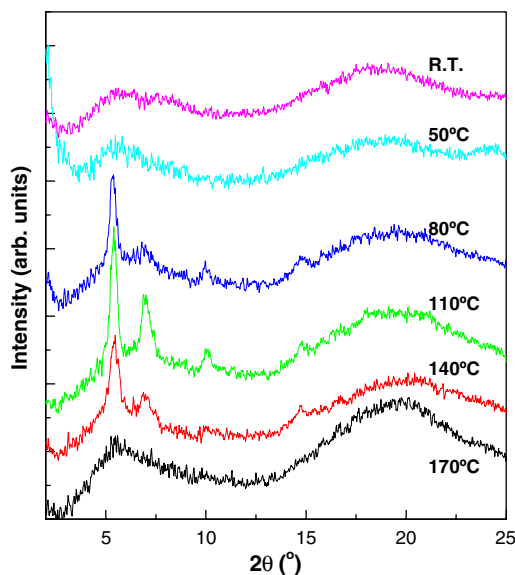


Fig. 4. XRD spectra of the pristine film (R.T.) and the films annealed at different temperatures.

of fwhm, 106 °C), the positions of the reflections remained almost unchanged, but their intensities were greatly enhanced. When further increasing the annealing temperature to 140 °C, the intensities of the scattering peaks started to gradually reduce, and finally the XRD pattern of the film annealed at 170 °C only showed two broad and diffused scattering peaks again, which was similar to the cases observed for the pristine film and the film annealed at 50 °C.

The PLM experiments further provided direct evidence of morphological changes for the pristine and annealed films, as shown in Fig. 5. No birefringence was observed under PLM for the pristine film (not shown here), indicating an amorphous morphology. When the annealing temperature (50 °C) was lower than the glass transition temperature, the film morphology hardly changed during thermal treatment (as shown in Fig. 5a). However, crystalline morphology was clearly observed for the film annealed at 80 °C (Fig. 5b) and 110 °C (Fig. 5c). And, nematic liquid crystalline texture appeared evidently in the films annealed at 140 °C (Fig. 5d) and 170 °C (Fig. 5e). These PLM observations are consistent with the above XRD results.

Obviously, annealing temperature easily affects the film morphology of PF6OC6. And the change of vibronic structure of the annealed films at different temperatures could be attributed to the difference or variation of the film morphology upon

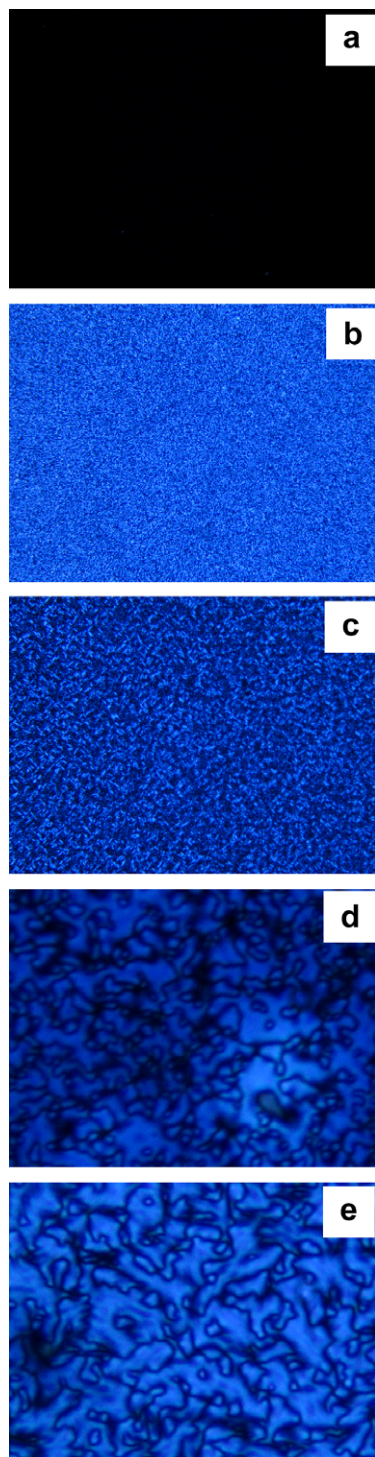


Fig. 5. PLM images (magnified 500 \times) of the films annealed at 50 °C (a), 80 °C (b), 110 °C (c), 140 °C (d) and 170 °C (e).

annealing. Thus, it could be proposed that the amount of vibronic structure of the PF6OC6 films

increases in the disordered state and decreases in the ordered state.

4. Conclusions

The phase transition of PF6OC6 during heating and cooling processes was investigated using DSC. The film morphology varied with different annealing temperatures. The annealed films exhibited amorphous state at 50 °C and above 170 °C, crystalline state at 80 °C, and nematic liquid crystalline state at 110 °C and 140 °C, respectively. The PLQE of the films hardly changes after annealing at different temperatures. The intensity of 0–1 emission relative to 0–0 emission and the fwhm of the spectra of the films firstly decreased and then increased with increasing annealing temperature. The vibronic structure is closely related to the film morphology of PF6OC6, and its intensity is enhanced in the disordered state and reduced in the ordered state.

Acknowledgements

This work was financially supported by the National Natural Science Foundation of China (Grant No. 50403012), the “Program for New Century Excellent Talents (NCET) in University” (Grant No. NCET-04-035), and the “Shanghai Rising-Star Program” (Grant No. 04QMX1403).

References

- [1] Tsumura A, Koezuka H, Ando T. *Appl Phys Lett* 1986;49(18):1210–2.
- [2] Garnier F, Hajlaoui R, Yassar A, Srivastava P. *Science* 1994;265(5179):1684–6.
- [3] Sirringhaus H, Wilson RJ, Friend RH, Inbasekaran M, Wu W, Woo EP, et al. *Appl Phys Lett* 2000;77(3):406–8.
- [4] Brabec CJ, Sariciftci NS, Hummelen JC. *Adv Funct Mater* 2001;11(1):15–26.
- [5] Kraft A, Grimsdale AC, Holmes AB. *Angew Chem Int Ed* 1998;37(4):402–28.
- [6] Friend RH, Gymer RW, Holmes AB, Burroughes JH, Marks RN, Taliani C, et al. *Nature* 1999;397(6715):121–8.
- [7] Misaki M, Ueda Y, Nagamatsu S, Yoshida Y, Tanigaki N, Yase K. *Macromolecules* 2004;37(18):6926–31.
- [8] Neher D. *Macromol Rapid Commun* 2001;22(17):1366–85.
- [9] Nguyen TQ, Martini IB, Liu J, Schwartz BJ. *J Phys Chem B* 2000;104(2):237–55.
- [10] Chen P, Yang GZ, Liu TX, Li TC, Wang M, Huang W. *Polym Int* 2006;55(5):473–90.
- [11] Donat-Bouillud A, Levesque I, Tao Y, D'Iorio M, Beaupre S, Blondin P, et al. *Chem Mater* 2000;12(7):1931–6.
- [12] Tapia MJ, Burrows HD, Valente AJM, Pradhu S, Scherf U, Lobo VMM, et al. *J Phys Chem B* 2005;109(41):19108–15.

- [13] Teetsov JA, Vanden Bout DA. *J Am Chem Soc* 2001;123(15):3605–6.
- [14] Gong X, Iyer PK, Moses D, Bazan GC, Heeger AJ, Xiao SS. *Adv Funct Mater* 2003;13(4):325–30.
- [15] Cao XY, Zhou XH, Zi H, Pei J. *Macromolecules* 2004;37(24):8874–82.
- [16] Zeng G, Yu WL, Chua SJ, Huang W. *Macromolecules* 2002;35(18):6907–14.
- [17] Yang GZ, Wu M, Wang M, Liu TX, Huang W. *Polymer* 2006;47(13):4816–23.
- [18] Chen P, Yang GZ, Wang CM, Wang WZ, Wang M, Liu TX. *Polym Int* 2007;56(8):996–1005.
- [19] Qu JQ, Zhang JY, Grimsdale AC, Mullen K, Jaiser F, Yang XH, et al. *Macromolecules* 2004;37(22):8297–306.
- [20] Zhu Y, Babel A, Jenekhe SA. *Macromolecules* 2005;38(19):7983–91.
- [21] Webster S, Batchelder DN. *Polymer* 1996;37(22):4961–8.
- [22] Tikhoplav RK, Hess BC. *Synth Met* 1999;101(1–3):236–7.
- [23] Liu B, Yu WL, Lai YH, Huang W. *Chem Mater* 2001;13(6):1984–91.
- [24] Yang GZ, Wang WZ, Wang M, Liu TX. *J Phys Chem B* 2007;111(27):7747–55.